

Optical distributed acoustic sensing based on the phase optical time-domain reflectometry

Shang Ying¹, Wang Chen¹, Liu Xiaohui¹, Wang Chang¹, Zhao Wen'an¹, Peng Gangding^{1,2}

(1. Shandong Key Laboratory of Optical Fiber Sensing Technologies, Laser Institute of Shandong Academy of Sciences, Jinan 250014, China; 2. School of Electrical Engineering & Telecommunications, University of New South Wales, NSW 2052, Australia)

Abstract: A distributed acoustic sensing (DAS) scheme was presented. Rayleigh backscattered light which contained acoustic signal induced phase changes along the sensing fiber was fed into a Michelson interferometer, the phase changes were demodulated by the Phase Generated Carrier technology. A piezoelectric simulation experiment of acoustic vibration was designed. The DAS system realized 10 m location resolution of the acoustic source, and the flat frequency response through the experiment.

Key words: distributed acoustic sensing; phase generated carrier; interferometer; frequency response

CLC number: TP212.1 **Document code:** A **DOI:** 10.3788/IRLA201746.0321003

基于相位光时域反射的光纤分布式声波传感研究

尚 盈¹, 王 晨¹, 刘小会¹, 王 昌¹, 赵文安¹, 彭刚定^{1,2}

(1. 山东省科学院激光研究所 山东省光纤传感重点实验室, 山东 济南 250014;
2. 新南威尔士大学 电气工程与电信学院, 澳大利亚 新南威尔士 2052)

摘要: 文中提出了一种光纤分布式声波传感方案。作用在传感光纤上的声波信号导致后向瑞利散射光的相位变化, 将含有声波信息的后向瑞利散射信号注入到迈克尔逊干涉仪, 并采用相位载波解调算法解调出相位信息。实验中采用压电拉伸器模拟声波振动, 分布式声波传感系统实现了 10 m 的空间分辨率以及平坦的频响。

关键词: 分布式声波传感; 相位载波; 干涉仪; 频响

收稿日期: 2016-07-10; 修订日期: 2016-08-20

基金项目: 国家自然科学基金(61605101); 山东省重点研发计划项目(2015GSF120001); 山东省重点研发计划项目(2014GGX103019)

作者简介: 尚盈(1981-), 男, 副研究员, 硕士, 主要从事光纤传感及系统设计方面的研究。Email: sy81012607@163.com

通信作者: 王昌(1977-), 男, 研究员, 博士, 主要从事智能材料与光纤传感技术方面的研究。Email: wang960100@163.com

0 Introduction

Long distance and wide range distributed acoustic signal monitoring is urgently needed in the field of marine oil, gas exploration and target detection. The unique advantage of optical fiber distributed sensing technology is that the fiber itself can act as the sensing element, so the distributed information of the whole sensing area can be measured in real time.

Optical fiber distributed sensing technology mainly consists of optical time/frequency domain reflection technology and optical fiber dual interferometer technology [1-2]. Optical time/frequency domain reflection (OTDR/OFDR) technology makes use of Rayleigh, Raman and Brillouin effects induced by external disturbance on the optical fiber [3]. Currently the Coherent optical time domain reflectometers (COTDR) [4-5], phase-sensitive OTDR (Φ -OTDR) [6-7] and Brillouin scattering [8-9] based sensors are effective technologies for vibration detection but not acoustic sensing which includes the information of the location, frequency, amplitude and phase. Dual interferometers have been developed to get the acoustic position and acoustic information (phase, amplitude and frequency) along the sensing fiber, such as Sagnac-Sagnac [8-9], Sagnac-MZ [10-11], Sagnac-Michelson [12] and MZ-MZ [13-14]. However the optical path design and demodulation algorithm of dual interferometers are complex, making it difficult to be implemented in practical application.

To sense the acoustic information, we proposed the optical fiber Distributed Acoustic Sensing (DAS) technology based on the coherent Rayleigh backscattering in the paper. In our experiment, the coherent light phase of the Rayleigh backscattering recorded acoustic information such as location, frequency, amplitude and phase. The DAS system has realized 10 m location resolution of the acoustic source, and the flat frequency response through the experiment.

1 Principle

1.1 Principle of Rayleigh backscattering

According to the measurement principle of one-dimensional impulse response model of the backscattering from a fiber, when we launch a coherent light pulse with pulse-width W and optical frequency ν into a fiber at $t=0$, we obtain a backscattered wave at the input end of the fiber which is given by [15-16]:

$$e_r(t) = \sum_{i=1}^N \alpha_i \exp(-\alpha \frac{c\tau_i}{n_f}) \exp\{j2\pi\nu(t-\tau_i)\} \text{rect}(\frac{t-\tau_i}{w}) \quad (1)$$

Where α_i and τ_i are the amplitude and delay of the i_{th} scattered wave respectively, N is the total number of scattering, α is the fiber attenuation constant, c is the velocity of light in vacuum, n_f is the refractive index of the fiber, and $\text{rect}(t-\tau_i)/w=1$, when $0 < (t-\tau_i)/w < 1$, and is zero otherwise. The delay τ_i corresponds to the distance z_i from the input end to the i_{th} scatterer through the relation $\tau_i = 2n_f z_i / c$. The term $\text{rect}(t-\tau_i)/w$ accounts for the change in the scattering volume seen as the pulse propagates.

As shown in Fig.1, when $e_r(t)$ is injected into the Michelson interferometer, we obtain two reflected waves at the coupler as shown in Fig.2.

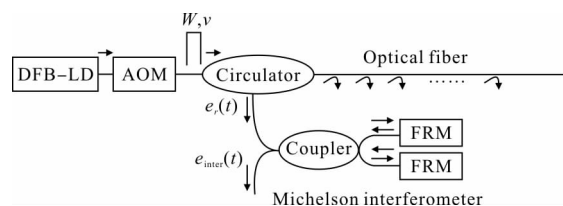


Fig.1 Optical path of self-interference principle of Rayleigh backscattering

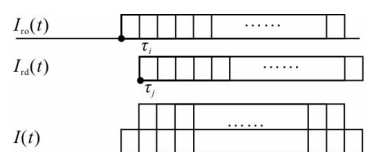


Fig.2 Self-interference schematic diagram of Rayleigh backscattering

The interferometer signal intensity $I(t)$ is given by:

$$I(t) = I_{in} + I_{in} = 2 \sum_{i=1}^N \sum_{j=1}^N \alpha_i \alpha_j \exp(-\alpha \frac{c(\tau_i + \tau_j)}{n_f}) \cos \varphi_{ij}$$

$$\text{rect}\left(\frac{t-\tau_i}{w}\right)\text{rect}\left(\frac{t-\tau_j}{w}\right) \quad (2)$$

where

$$I_m = \sum_{i=1}^N \alpha_i^2 \exp(-2\alpha \frac{c\tau_i}{n_f})$$

$$I_n = \sum_{j=1}^N \alpha_j^2 \exp(-2\alpha \frac{c\tau_j}{n_f})$$

$$\varphi_{ij} = \tau_i - \tau_j = \frac{4\pi v n_f}{c} (z_i - z_j)$$

As shown in Eq.(2), it is known that the interference signal contains phase information φ_{ij} induced by the acoustic signal, so as long as phase information φ_{ij} can be demodulated, the relevant information such as the acoustic signal amplitude, phase and frequency can be restored.

1.2 Modulation and demodulation techniques of phase generated carrier

Interferometer output signal I can be expressed as

$$I = A + B \cos[C \cos \omega_0 t + \phi(t)] \quad (3)$$

Where A is the average optical power of interferometer output signal, $B = \kappa A$, $\kappa \leq 1$ and κ is interference fringe visibility, $C \cos \omega_0 t$ is phase generated carrier, $\phi(t) = D \cos \omega_s t + \psi(t)$, $D \cos \omega_s t$ is phase change induced by the tested signal, $\psi(t)$ is slow variation of the initial phase caused by environment.

Equation(3) can be expressed with Bessel function expansion:

$$I = A + B \{ [J_0(C) + 2 \sum_{k=0}^{\infty} (-1)^k J_{2k}(C) \cos 2k\omega_0 t] \cos \phi(t) - 2 [\sum_{k=0}^{\infty} (-1)^k J_{2k+1}(C) \cos(2k+1)\omega_0 t] \sin \phi(t) \} \quad (4)$$

As shown in Fig.3, the signal I propagate through this process, so the final output of the system which contains the tested signal $D \cos \omega_s t$ is

$$B^2 G H J_1(C) J_2(C) D \cos \omega_s t \quad (5)$$

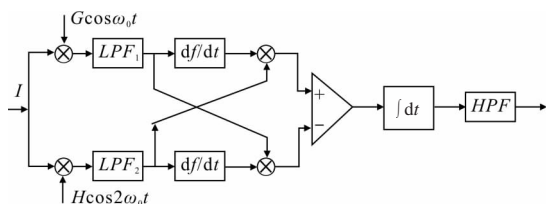


Fig.3 PGC demodulation scheme

Where G and H is the amplitude of fundamental and double frequency signal, respectively.

2 Experiment

2.1 DAS experiment system design

DAS experiment system diagram is shown in Fig.4. Distributed-feedback laser diode (DFB-LD) with narrow line width of 5 kHz is used as light source, CW light is modulated into sequence of pulses by acoustic-optic modulator (AOM). Those pulses have repetition rate (f) of 20 kHz and pulse-width(W) of 100 ns, then the modulated pulses are amplified by Erbium-doped fiber amplifier (EDFA), the output of EDFA is filtered by a narrow-band filter to remove spontaneous emission. The modulated pulses are gated into 500 m sensing fiber by a circulator, in the experiment, 10 m of fiber is wrapped around the PZT to simulate the vibration signal caused by sound waves and when the sensing fiber detects acoustic wave, the phase information of Rayleigh backscattered light changes, the Rayleigh backscattered light is then split into two beams by a 3 dB fiber coupler(50:50), the one part is modulated by Phase Modulator (PM) with 40 kHz frequency, then interference light is amplified by an EDFA, filtered and then received by a Photoelectric Detector (PD) to produce the electrical signal that contains the coherent light information of the Rayleigh scattering, this signal is demodulated by PGC module and then acquired with PC with 100 MHz sampling rate.

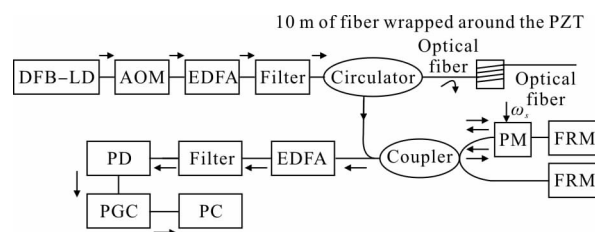


Fig.4 DAS detection system block diagram

2.2 DAS experiment result and discussion

During the experiment, a fixed amplitude of 3 V sinusoidal signal with the frequency range from 100 Hz

to 900 Hz was respectively fed to the PZT, the fiber wrapped around the PZT detected the signal, whose position is about from 225 m to 235 m away the circulator.

Figure 5 is the three-dimensional intensity demodulation figure with the frequency of 600 Hz, we obtained propagating signals at the range from 225 m to 235 m of the sensing fiber. The propagating signals are superimposed and averaged, then the demodulation results of time domain is shown in Fig.6. The amplitude of 600 Hz is calculated by the fast Fourier transform (FFT) spectrum analysis, as shown in Fig.7, amplitude is 0.94 V, and SNR of the spectrum is 40dB.

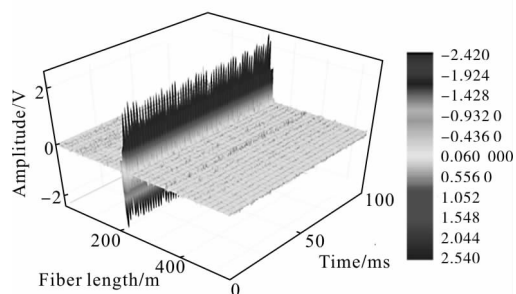


Fig.5 DAS demodulation result of a 600 Hz signal

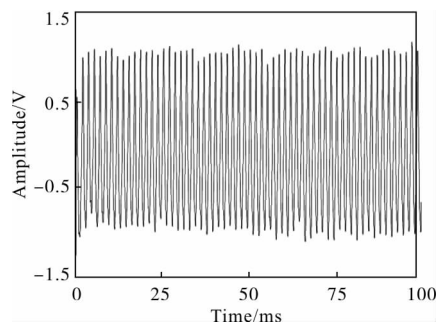


Fig.6 DAS demodulation result in time domain

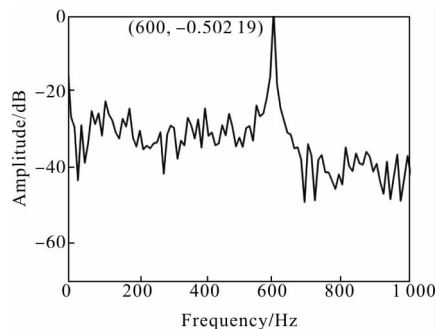


Fig.7 DAS demodulation result in frequency domain

Demodulation results of other frequency are shown in Fig.8 by the same method. The maximum

variation of the amplitude is almost 0.2 dB from 100 Hz to 900 Hz.

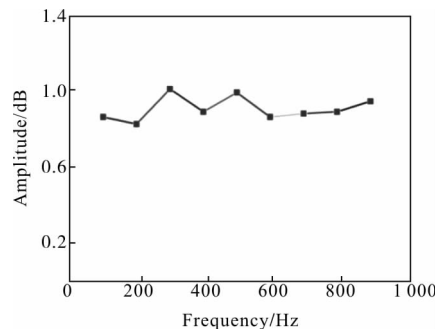


Fig.8 DAS frequency response

The spatial resolution S_R of DAS system is related the pulse width W and the sampling rate (Mbps) S_a :

$$S_R = \max(2n_f W/c, c/2S_a n_f) \quad (6)$$

Where c is the light speed; n_f is the refractive index of the fiber.

According to Eq. (6), the value of spatial resolution is decided by the maximum between $2n_f W/c$ and $c/2S_a n_f$. In our system, $W=100$ ns, $S_a=100$ Mbps, so $S_R=10$ m.

The external sound pressure P acting at the L meter length of the fiber can induce the phase changes $\Delta\phi$:

$$\frac{\Delta\phi}{P} = \frac{L\pi}{\lambda E} (4n_f \mu + 3n_f^3 \mu p_{12} - n_f^3 p_{11}) \quad (7)$$

Where n_f is the refractive index of the fiber, λ is the wavelength of light, p_m is the elastic coefficient, E is the elastic coefficient, μ is the Poisson's ratio.

According to Eq.(7), the sensitivity of the DAS system is related to the property of the fiber, the wavelength of light.

3 Conclusion

An optical fiber distributed acoustic sensing technology based on the self-interference of Rayleigh backscattering is demonstrated. Our experiment proves that the scheme can restore the acoustic information with the single-mode fiber, we realized the 10 m location resolution of the acoustic source and the flat

frequency response through the experiment. This work provides basis on further study and performance improvement

References :

- [1] Sergi Villalba, Joanr Casas. Application of optical fiber distributed sensing to health monitoring of concrete structures [J]. *Mechanical Systems and Signal Processing*, 2013, 39: 441-451.
- [2] Yan Bing, Dong Fengzhong. Application of pipeline safety real-time monitoring with distributed optical fiber sensing technique based on coherent Rayleigh backscattering [J]. *Chinese Journal of Quantum Electronics*, 2013, 30(3):341-347.
- [3] Bao Xiaoyi, Chen Liang. Recent progress in distributed fiber optic sensors[J]. *Sensors*, 2012, 12: 8601-8639.
- [4] Lu Yuelan, Zhu Tao. Distributed vibration sensor based on cCoherent detection of phase-OTDR [J]. *Journal of Light Wave Technology*, 2010, 28(22): 3243-3248.
- [5] Yahei Koyamada. Fiber-optic distributed strain and temperature sensing with very high measurand resolution over long range using coherent OTDR [J]. *Journal of Light Wave Technology*, 2009, 27(9): 1142-1145.
- [6] Tu G J, Zhang X P, Zhang Y X. The development of an Φ -OTDR system for quantitative vibration measurement[J]. *Journal of Light Wave Technology*, 2015, 27(12): 1349-1352.
- [7] Zhou L, Wang F, Wang X C. Distributed strain and vibration sensing system based on phase-sensitive [J]. *IEEE Photonics Technology Letters*, 2015, 27(17): 1884-1887.
- [8] Zhang G, Xi C, Liang Y. Dual-Sagnac optical fiber sensor used in acoustic emission source location [C]// IEEE Conference on Cross Strait Quad-Regional Radio Science and Wireless Technology, 2011, 2: 1598-1602.
- [9] Bian Pang, Wu Yuan, Jia Bo. Dual-wavelength Sagnac interferometer as perimeter sensor with Rayleigh backscatter rejection[J]. *Optical Engineering*, 2014, 53(4): 044111.
- [10] Chen Qingming, Jin Chao. A distributed fiber vibration sensor utilizing dispersion induced walk-off effect in unidirectional Mach-Zehnder interferometer [J]. *Optics Express*, 2014, 22(3): 2167-2173.
- [11] Wei Pu, Shan Xuekang, Sun Xiaohan. Frequency response of distributed fiber-optic vibration sensor based on nonbalanced Mach-Zehnder interferometer [J]. *Optical Fiber Technology*, 2013, 19: 47-51.
- [12] Kondrat M, Szustakowski M, Palka N. A Sagnac-Michelson fibre optic interferometer: Signal processing for disturbance localization[J]. *Opto-electronics Review*, 2007, 15(3): 127-132.
- [13] Li J, Ning T, Pei L. Photonic generation of triangular waveform signals by using a dual-parallel Mach-Zehnder modulator[J]. *Optics Letters*, 2011, 36(19): 3828-3830.
- [14] Jiang Lihui, Yang Ruoyu. Identification technique for the intrusion of airport enclosure based on double mach-zehnder interferometer[J]. *Journal of Computers*, 2012, 7(6): 1453-1458.
- [15] Masataka Nakazawa. Rayleigh backscattering theory for single-mode optical fibers [J]. *J Opt Soc Am*, 1983, 73(9): 1175-1180.
- [16] Juskaitis R. Interferometry with Rayleigh backscattering in a single-mode optical fiber [J]. *Optics Letters*, 1994, 19(3): 225-227.